the uncertainties compared with the errors in t and H_{res} obtained from the statistical analysis of the data. Consequently, we believe that the results of the present investigation represent the most accurate values of the Fermi-surface caliper dimensions yet obtained for molybdenum.

In conclusion, we report accurate measurements of caliper dimensions of the molybdenum Fermi surface in the $\langle 110 \rangle$ plane. From these measurements, the separation between the jack and octahedra is estimated to be 7.5% of the ΓH dimension, which implies an unexpectedly large spin-orbit interaction in metallic molybdenum. A detailed discussion of these results together with the experimental technique will be published elsewhere.

We would like to thank Professor T. K. Wagner and Professor L. Hodges for many valuable discussions. The technical assistance of J. S. Hartman and H. H. Baker is gratefully acknowledged.

*Work performed at the Ames Laboratory of the U. S. Atomic Energy Commission.

†National Defense Education Act Title IV Predoctoral Trainee 1968-1969. Present address: Department of Physics, Michigan State University, East Lansing, Mich. 48823.

[1]T. L. Loucks, Phys. Rev. 139, A1181 (1965).
[2]W. M. Lomer, Proc. Phys. Soc. (London) 84, 327 (1964).
[3]W. M. Walsh, Jr., and C. C. Grimes, Phys. Rev. Letters 13, 523 (1963).
[4]L. F. Mattheiss and R. E. Watson, Phys. Rev. Letters 13, 526 (1964).
[5]V. V. Boiko, V. A. Gasparov, and I. G. Gverdtsiteli, Zh. Eksperim. i Teor. Fiz. 56, 489 (1969) [Soviet Phys. JETP 29, 267 (1969)].
[6]G. Leaver and A. Myers, Phil. Mag. 19, 465 (1969).
[7]V. F. Gantmakher, Zh. Eksperim. i Teor. Fiz. 44, 811 (1963) [Soviet Phys. JETP 17, 549 (1963)].
[8]The indicated uncertainty represents a 90% confidence limit determined from a statistical analysis of the data.
[9]J. F. Koch and T. K. Wagner, Phys. Rev. 151, 467 (1966).
[10]I. P. Krylov and V. F. Gantmakher, Zh. Eksperim. i Teor. Fiz. 51, 740 (1966) [Soviet Phys. JETP 24, 492 (1967)].
[11]R. Herrmann, Phys. Status Solidi 25, (1968).

INFLUENCE OF LATTICE CONTRACTION ON LONG-RANGE ORDER IN CoO NEAR T_N

M. D. Rechtin, S. C. Moss, and B. L. Averbach
Department of Metallurgy and Materials Science, Center for Materials Science and Engineering, Massachusetts Institute of Technology, Cambridge, Massachusetts 02139
(Received 16 April 1970)

Just below the Néel temperature of CoO, the intensity of neutrons scattered by the antiferromagnetic lattice of Co^{2+} ionic spins should vary as $I \propto (T_N - T)^{2\beta}$. We measure $\beta = 0.244 \pm 0.015$, or substantially lower than the Ising prediction of 0.3125 which CoO should assume. By applying a phenomenological correction for the measured tetragonal lattice contraction below T_N, similar in form to Heller's correction for the contraction in MnF_2, we make $T_N = T_N(T)$ which raises β to a value of 0.290 ± 0.025. By thus adjusting for nonrigidity of the lattice we bring β into a range which includes the rigid-lattice Ising prediction.

Below its Néel temperature ($T_N \cong 289°K$) CoO undergoes a phase transition from a paramagnetic to antiferromagnetic state. The change is accompanied by a tetragonal contraction with $c/a = 0.988$ at 93°K[1,2] and a small trigonal elongation of $e_{yz} = e_{zx} = e_{xy} = 5 \times 10^{-4}$.[3] Precise dilatometry measurements of the behavior of the tetragonal contraction in our single crystal indicate a continuous change of lattice dimensions on passing through the critical temperature. Neutron diffraction measurements of magnetic peak positions show this same characteristic as do the measurements of sublattice magnetization reported here.

Consequently, the phase transition appears to be of order greater than unity. The Co^{2+} ionic spins order ferromagnetically within any single $\{111\}$ plane while each $\{111\}$ plane is oriented antiferromagnetically with respect to the two adjacent planes. This configuration signifies a predominantly next-nearest-neighbor (nnn) exchange interaction. The 6 nnn ionic moments are oriented antiparallel while of the 12 nearest neighbors (nn), half are parallel and half antiparallel. In a study to be reported elsewhere our measurements of the critical scattering above T_N suggest, via an analysis similar to the Clapp-Moss treatment,[4] that the nn exchange in-

teraction is about one-third to one-half the value of the nnn energy. Although a number of noncollinear spin-axis structures are possible in CoO,[5,6] present experimental evidence points to a collinear structure[7] with the moments tipped out of the {111} planes 7°50′ toward the c axis.[6] This spin-axis orientation was verified by our single-crystal measurements. We also noted that the spin axis does not change orientation with temperature from measurements at 4.2 and 272°K.

Here we shall describe for CoO the decay of antiferromagnetic long-range order in the critical region in terms of the critical exponent, β. The spontaneous sublattice magnetization in the critical region is given by $M(T)/M(0) = D(1-T/T_N)^{\beta}$. The neutron scattering cross section (or scattered intensity, I) is proportional to the square of the magnetization and thus we may determine 2β from $I = C(T_N - T)^{2\beta}$ much as has been done in other studies of Ising and Heisenberg systems.[8] In order to compare any experimental β value with a Heisenberg or Ising model we must, however, have the system referred to its rigid-lattice state. Essam and Baker[9] have recently developed the effects of lattice compressibility on critical behavior, and current work of Norvell and Als-Nielsen[10] on long-range order in β'-CuZn showed agreement with the compressible bcc lattice calculations, although this result has recently been questioned by Chipman and Walker.[11] We have here measured the decay of spontaneous sublattice magnetization in the critical region for CoO by neutron diffraction and find a β of about $\frac{1}{4}$. By correcting for the lattice compressibility, however, an Ising-like β is obtained and this agrees with the treatment of Salamon[12] who shows that for CoO the behavior should become Ising-like for $(1-T/T_N) \lesssim 0.020$. His specific-heat measurements support this conclusion by yielding nearly Ising values for the C_v indices α and α' of 0.12 and 0.05, respectively.

In our experiment neutrons of $\lambda = 1.05$ Å were obtained by transmission from the (111) planes of a mosaic lead single crystal. After monochromatization the beam was collimated by a cadmium slit system with horizontal divergence of 3.2′. The $\frac{1}{2}\lambda$ neutrons were then removed by a Pu^{239} filter, and the neutron beam was diffracted from the CoO single crystal into a BF_3 counter with open collimation. The crystal itself was nearly spherical in shape with a mean diameter of 0.68 cm. The mosaic width of the crystal was 7.1′. Chemical analysis of the specimen showed the Co^{2+} to O^{2-} ratio was 1.001 to 1.000 with a 0.15% Ni^{2+} impurity. The specimen was held in an aluminum clamp attached to a two-circle goniometer, and this assembly was mounted within a cryostat. Temperature was controlled to ±0.05°K with an ice water bath in the liquid nitrogen reservoir and a 5-W heater in the sample chamber. The (111) magnetic peak intensity was measured by a rotating crystal (ω) scan with the peak height being used to characterize the decay of magnetization. Since only the long-range order is varying in the system, the peak breadth remains constant and $M(T)/M(0)$ is still proportional to $I^{1/2}$. However we cannot compare the peak heights of several reflections since instrumental factors invalidate peak height as an absolute measurement.

Nuclear and magnetic multiple-scattering contributions were avoided by first calculating the positions in azimuthal angular setting of the crystal that are free from them. The temperature diffuse scattering (TDS) correction was evaluated on the basis of the Debye-Waller factor for CoO. From measurements of the mean-square vibrational amplitude of the Co^{2+} ion in CoO at room temperature,[13] the Debye-Waller factor e^{-2w} is about 0.991 for the (111) reflection near room temperature. This indicates that much less than 1% of the measured radiation is thrown back into the (111) reflection in the TDS process. We therefore assume a negligible correction for TDS.

Secondary extinction can be an important correction in a highly mosaic single crystal for high-intensity Bragg reflections. In weakly scattering processes, such as critical scattering, there is no extinction. To be free of secondary extinction the measured intensity must be given by the ideally mosaic crystal formula, namely I is proportional to the square of the structure factor. For the given experimental conditions we plotted the integrated intensities for a number of nuclear reflections against the ideal mosaic prediction. From this it was determined that there would be negligible extinction for all but the lowest three temperatures in our long-range-order study. In fact, however, the measured integrated magnetic intensities all fell on the extrapolation of the extinction-free line, indicating the absence of both primary and secondary extinction. The reason for this lies in the presence of the so-called "S" or spin domains in CoO. Upon ordering below T_N, spontaneous magnetization can begin on any one of the four {111} planes with equal probability because the tetragonal contrac-

Table I. Summary of data and corrections on long-range-order measurements in CoO.

T(°K)	<I>	n	σ(I)	I_{BG}	I_{CS}	I_{BRAGG}	w
278.2	21503	1	146	134	62	21307	3.56
284.4	14623	1	121	134	308	14181	2.73
285.0	13336	6	47	134	328	12874	3.02
285.1	13467	1	116	134	333	13000	2.83
285.8	12149	3	64	134	357	11658	1.75
286.0	11821	11	33	134	367	11320	6.41
287.3	9023	4	47	134	422	8467	2.91
287.5	8617	2	66	134	432	8051	2.43
288.7	4352	19	15	134	550	3715	1.00
288.8	3363	5	25	134	623	2606	0.65
288.9	2940	5	31	134	825	1981	0.38

tion axis is symmetric with respect to these four {111} planes. Thus, there are four distinct domains below T_N with their overall volumes equal.[14] We have also verified this to be so by measurements on the four {333} planes at approximately 100°K. This domain formation results in a distribution of domains much smaller in volume than the perfect mosaic regions and renders all magnetic reflections extinction free.

Besides the "S" domains we can have "T" domains, that is, regions of the crystal with different contraction c axes. Uchida et al.[15] have shown that application of a temperature gradient along one of the ⟨001⟩ directions upon passing through T_N causes most contractions to occur along one axis. For our set of measurements we obtained 96% of one "T" domain. For any case, in the temperature region of our measurements for determining β, the (111) peak splitting due to the three domains was very small so that no correction of intensity was needed and our use of peak height was not invalidated.

To accomplish the removal of the critical scattering contribution below T_N, the (111) position was scanned at a number of temperatures above T_N. The wings of the peak profiles below T_N, free from Bragg intensity, were matched with the diffuse peak from above T_N which had the best fit of intensity and curvature. This diffuse peak was then used as the critical scattering correction. The temperature dependence of the (111) peak intensity below T_N is summarized in Table I. This table gives the temperature of the measurement, T(°K); average intensity for n repetitions, $\langle I\rangle$; the expected Poisson standard deviation, $\sigma(I)$; background intensity, I_{BG}; critical scattering correction, I_{CS}; corrected long-range order intensity, I_{BRAGG}; and the statistical weight w of the observation relative to the measurement at $T = 288.7$°K with unit weight. A weighted least-squares fit (LSF) was carried out to find the parameter β for various values of T_N. The best fit was determined by finding the minimum of the sum of the squares of the standard deviations, $S^2(T_N) = \sum_T w(T)[I_{BRAGG}(T) - C(T_N - T)^{2\beta}]^2$. A typical double-log plot of the Bragg intensity versus $T_N - T$ is shown in the upper line in Fig. 1 for the best T_N. There appears to be no systematic deviation from a straight line throughout the entire temperature range, indicating again that no secondary extinction is present. The lower line in Fig. 1 is the result of correcting for lattice contraction and is discussed below.

This value for β (~0.25) is surprisingly small. On the basis of Salamon's specific-heat measurements we would expect an Ising value near $\frac{5}{16}$. A major correction to our measured β was therefore suspected to be the lattice compressibility, since the tetragonal distortion is extremely large. The effect of pressure on the Néel temperature has been determined by Bloch, Chaisse, and Pauthenet.[16] They found, $dT_N/dP = 0.60$°K kbar^{-1} and for $T_N = 288.9825$°K, $(1/T_N)(dT_N/dP) = (d\ln T_N)/dP = 2.076 \times 10^{-3}$ kbar^{-1}. The depen-

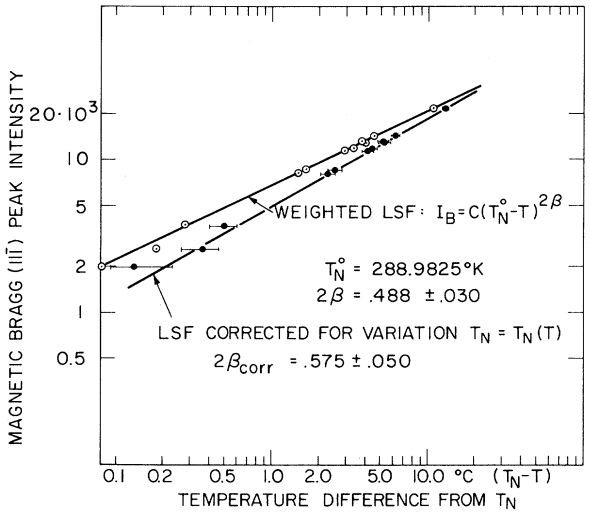

FIG. 1. Double-log plot of magnetic Bragg peak intensity from the (111) planes in CoO versus the temperature difference $(T_N - T)$. The upper limit is a least-squares fit (LSF) to a power law assuming a constant $T_N{}^0$. The fit was made without the first two points near $T_N{}^0$ and the resulting line still includes them indicating that the large critical scattering correction near $T_N{}^0$ was appropriate. The lower line is a similar plot in which the simple variation of $T_N(T)$ was applied and where the error bars are all due to the uncertainty in $T_N(T)$.

dence of the c-axis length on pressure was found from the compressibility, $[1/c(T_N)]dc/dP = d\ln c/dP = -0.605\times10^{-3}$ kbar^{-1}, thus $(1/T_N)(dT_N/dP)/[1/c(T_N)]dc/dP = d\ln T_N/d\ln c = -3.43$. Expressing the variation of T_N with the c axis, $T_N(T) = T_N{}^0\{1-3.43[c(T)-c(T_N)]/c(T_N)\}$. Knowing $\Delta c/c$ from strain measurements on our crystal (Fig. 2), we may determine T_N as a function of temperature. If we now account for the increase of T_N with decreasing temperature in Fig. 1, we must shift the coordinate $(T_N - T)$ of each point. Upon doing this we note a change of β to 0.290 ± 0.025. The shift is made with respect to $T_N{}^0$, the temperature at which the long-range order goes to zero. The value of 288.9825°K obtained in the LSF is within ±0.1°K of the absolute T_N, and this error is included in the error brackets of the corrected data points.

Another approach to correct for the lattice compressibility is taken from Heller[17] in his NMR study of MnF_2 in which we express the intensity in terms of the reduced temperature and $T_N(T)$, $I^{1/(2\beta)}/T_N(T) = A(T)^{1/(2\beta)} - A(T)^{1/(2\beta)}T/T_N(T)$. The β value which linearizes this equation gives the best fit. A plot of the left side of the equation is made against $T/T_N(T)$. Then a

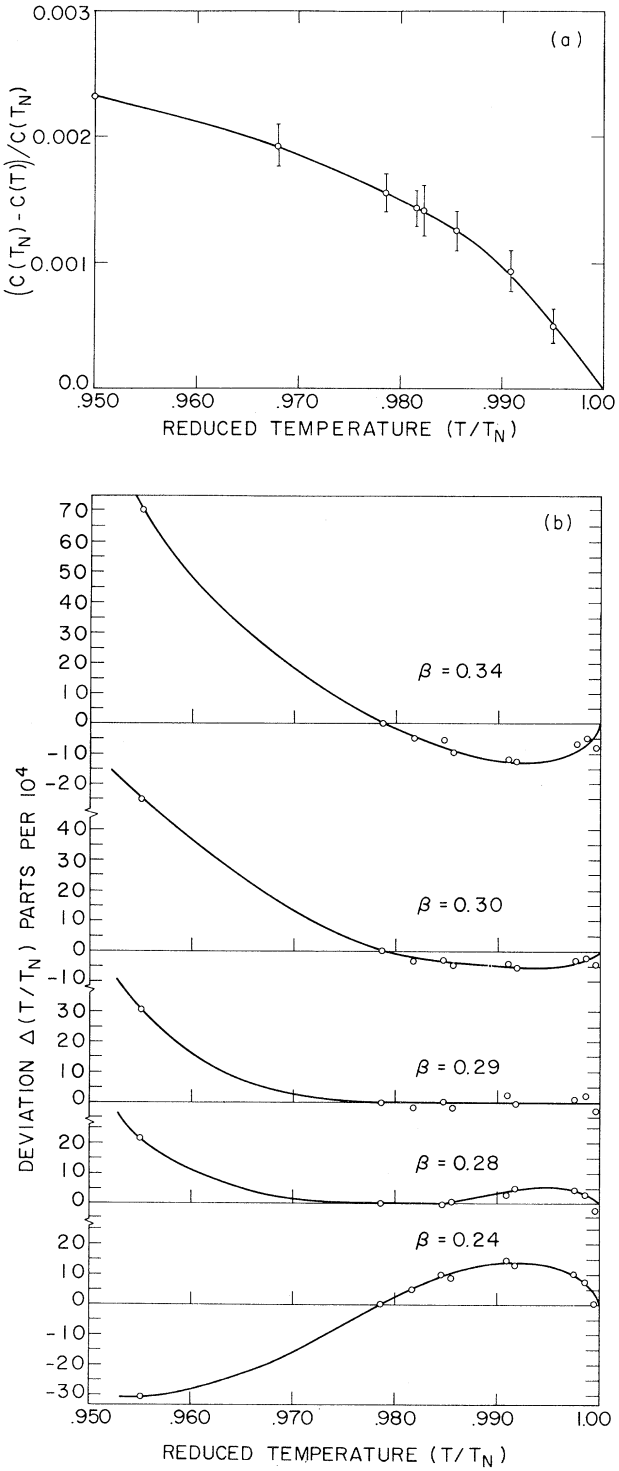

FIG. 2. (a) The variation of the tetragonal c parameter $\Delta c/c$ as a function of reduced temperature T/T_N. (b) The deviation from linearity of the plot of $I^{1/(2\beta)}/T_N(T)$ vs $T/T_N(T)$ for five different β values. This deviation is expressed in terms of separation along the $T/T_N(T)$ coordinate. The appropriate β value leads to no departure.

straight line is plotted through $T/T_N=1.000$ and (somewhat arbitrarily, although it makes little difference) the data point at $T=284.4°K$ for a number of β values. The deviation of the data points from this straight line is given in the lower part of Fig. 2 for five different β values. The best fit is for $\beta \cong 0.29$ which is the same conclusion found by correcting Fig. 1. Within experimental accuracy, set mainly by the tetragonality data, the β thus appears to assume an Ising value in agreement with the experimental specific-heat measurements in the critical region.[12]

We would especially like to thank Professor H. E. Stanley for many helpful discussions and for showing that the simple shift in $T_N(T)$ included in Fig. 1 gives the same result as Fig. 2. We are also indebted to M. B. Salamon for discussions of his work and ours and for his preprint. We would in addition like to thank J. Als-Nielsen, R. Harrison, L. P. Kadanoff, and C. B. Walker for stimulating discussions. This work was supported by the National Science Foundation to whom it is a pleasure to express our appreciation.

[1]H. P. Rooksby, Acta Cryst. 1, 226 (1948).
[2]R. C. Lambs and H. P. Rooksby, Nature 165, 442 (1950).
[3]J. Nagamiya, S. Saito, Y. Shimomura, and E. Uchida, J. Phys. Soc. Japan 20, 1285 (1965).
[4]P. C. Clapp and S. C. Moss, Phys. Rev. 142, 418 (1966); 171, 754 (1968).
[5]W. L. Roth, Phys. Rev. 111, 772 (1958).
[6]B. van Laar, Phys. Rev. 138, A584 (1965).
[7]S. Saito, K. Nakahigashi, and Y. Shimomura, J. Phys. Soc. Japan 21, 850 (1966).
[8]J. Als-Nielsen and O. W. Dietrich, Phys. Rev. 153, 717 (1967), on β'-CuZn; L. M. Corliss, A. Delapalme, J. M. Hastings, H. Y. Lau, and R. Nathans, J. Appl. Phys. 40, 1278 (1969), on $RbMnF_3$; J. C. Norvell, W. P. Wolf, L. M. Corlis, J. M. Hastings, and R. Nathans, Phys. Rev. 186, 557 (1969), on DyAlG where $\beta \cong \frac{1}{4}$ due to long-range dipolar forces. This is discussed at greater length by N. E. Frankel and A. E. Spargo, Phys. Letters 31A, 442 (1970).
[9]G. A. Baker, Jr., and J. W. Essam, Phys. Rev. Letters 24, 447 (1970).
[10]J. C. Norvell and J. Als-Nielsen, to be published.
[11]D. R. Chipman and C. B. Walker, Bull. Am. Phys. Soc. 15, 363 (1970).
[12]M. B. Salamon, to be published.
[13]R. Uno, J. Phys. Soc. Japan 18, 1686 (1963).
[14]B. van Laar, Phys. Rev. 141, 538 (1966).
[15]E. Uchida, R. Fukuoka, H. Kondoh, J. Takeda, Y. Nakazumi, and J. Nagamiya, J. Phys. Soc. Japan 19, 2088 (1964).
[16]D. Bloch, F. Chaisse, and R. Pauthenet, J. Appl. Phys. 37, 1401 (1966).
[17]P. Heller, Phys. Rev. 146, 403 (1966).

MACROSCOPIC AND MICROSCOPIC THEORIES OF DIPOLE-EXCHANGE SPIN WAVES IN THIN FILMS: CASE OF THE MISSING SURFACE STATES

T. Wolfram and R. E. De Wames
Science Center, North American Rockwell Corporation, Thousand Oaks, California 91360
(Received 18 March 1970)

Calculations of dipole-exchange spin waves in thin films using a microscopic model show no evidence of surface modes above the lowest bulk frequency, in contrast to recent results based on a macroscopic model. The apparent absence of the surface branch in the former model is explained in terms of the admixture of bulk and surface waves. Nearly exact quantitative agreement between the two models is obtained for wave vectors as large as 10^7 cm^{-1}.

A simple ferromagnetic insulator is characterized by short-range exchange interactions and long-range dipole-dipole interactions. The Heisenberg exchange model (valid for large wave vectors) predicts surface spin-wave modes with frequencies below the bulk modes.[1-3] In contrast, magnetostatic theory (valid for small wave vectors) includes only dipolar effects and predicts a spin-wave surface mode above the lowest bulk frequency.[4] The behavior of surface and bulk spin waves in the transition region for which both dipolar and exchange effects are important has been a subject of considerable interest recently.[5-13] Mills[14] stated that the magnetostatic Damon-Eshbach (DE) surface branch would decrease with increasing wave vector and exit below the bulk band to join smoothly with the Heisenberg surface branch. The results of a microscopic theory in which the discrete exchange and dipolar interactions of a 30-atomic-layer system were numerically calculated were reported by Benson and Mills[8] (BM). These authors reported that